Processing and Application of Ceramics 12 [4] (2018) 335–341
https://doi.org/10.2298/PAC1804335Z



# Influence of Co ion doping on the microstructure, magnetic and dielectric properties of $Ni_{1-x}Co_xFe_2O_4$ ceramics

Jihua Zou[1,2], Rongli Gao[1,2,*], Chunlin Fu[1,2], Wei Cai[1,2], Gang Chen[1,2], Xiaoling Deng[1,2]

[1]*School of Metallurgy and Materials Engineering, Chongqing University of Science and Technology, Chongqing 401331, China*
[2]*Chongqing Key Laboratory of Nano/Micro Composite Materials and Devices, Chongqing 401331, China*

Received 25 June 2018; Received in revised form 30 September 2018; Accepted 11 November 2018

## Abstract

*$Ni_{1-x}Co_xFe_2O_4$ (x = 0, 0.2, 0.4, 0.6, 0.8) ceramics were prepared by chemical co-precipitation method and the effect of Co ion doping on the microstructure, magnetic and dielectric properties has been investigated. The results show that the synthesized ceramics display only spinel phase of $Ni_{1-x}Co_xFe_2O_4$, without other apparent impurities found. The lattice of $Ni_{1-x}Co_xFe_2O_4$ crystal structure was distorted as a result of the incorporation of Co ion, and the lattice parameters increase with the increase of Co ion content. The grain size decreases slightly with increasing the content of Co ion, indicating a change of particle size and morphology at higher doping content. The results of impedance analysis shows that the sample doped with 80 at.% Co possesses the maximal dielectric constant, while the pure $NiFe_2O_4$ sample shows the minimal value when the frequency is below 0.1 MHz. The M-H loops of these ceramics exhibit highly magnetic nature and the saturation magnetization. The remnant magnetization increases linearly with the increase of Co-concentration in nickel ferrite while the coercive field ($H_c$) shows non-monotonic variation with Co content. The minimal and maximal values of $H_c$ can be obtained when the Co concentrations are 40 and 80 at.%, respectively. The highest value of the saturation magnetization is 63 emu/g obtained with 80 at.% Co doping while the lowest value is ~31 emu/g for the pure $NiFe_2O_4$ ceramics. The abnormal magnetic behaviour is due to the A-B super exchange interaction when magnetic $Co^{2+}$ ions are added.*

***Keywords:*** *Ni-Co ferrites, microstructure, dielectric properties, magnetic properties*

## I. Introduction

Spinel ferrites $MFe_2O_4$ (M = Mg, Cu, Ni, Co, Mn, Zn, etc.) have attracted extensive attention in the past few decades not only due to their interesting properties, such as specific magnetization, magneto crystalline anisotropy, high electrical resistivity, high Curie temperature and chemical stability [1–3], but also because of their broad applications in catalysis, high density information recording, magnetic storage, energy storage, biological applications and ferrofluid technology as carriers for magnetically guided drug delivery and ferrofluid seal [4–10]. Among them, $CoFe_2O_4$ is one of the most important ferrites because of its perfect magnetic properties, excellent thermal stability and high anisotropy field [11–14]. Another typical ferrite is $NiFe_2O_4$ due to its ferromagnetic properties, low electrical conductivity and thus low eddy current losses and high electrochemical stability [15–18]. In addition, $CoFe_2O_4$ belongs to the class of hard magnetic materials, which exhibits very high value of saturation magnetization and coercive field, whereas $NiFe_2O_4$ is soft magnetic material having low saturation magnetization and coercivity. As a consequence, one can speculate that with the substitution of Co ions in $NiFe_2O_4$ lattice, the obtained magnetic compound will have the characteristic of both spinels, which encourages their use in many other potential applications. They have the advantage of tuning and tailoring their physical properties by changing the chemical composition, grain size, morphology and lattice strain [19–23]. The exploration of various combinations of different magnetic materials may improve their physical properties and provide a better fundamental un-

*Corresponding authors: tel: +86 23 65023479,
e-mail: *gaorongli2008@163.com*

derstanding of the magnetic interactions and achieve desirable specific applications [24–27]. According to the exchange-coupling theory, nanocomposite permanent material can have the high remanence of soft phase and the high coercivity of hard phase at the same time.

Therefore, it is very important and necessary to tailor the physical properties of ferrite ceramics based on the application requirements which can be achieved by adjusting the concentration of cobalt and nickel magnetic phases in these materials. Obviously, on account of such interesting and useful properties, it is of great significance to carry out in-depth investigation on the preparation procedures and characterization analysis. The purpose of this work is to describe the synthesis of the single phase Co-doped $NiFe_2O_4$ ceramics by chemical co-precipitation method and to characterize high coercive field/low coercive field magnetic composites by various analytical techniques in order to investigate the structure, morphology, dielectric and magnetic properties.

## II. Experimental procedure

$Ni_{1-x}Co_xFe_2O_4$ particles with different compositions ($x$ = 0, 0.2, 0.4, 0.6, 0.8) were synthesized by the chemical co-precipitation method. Aqueous solutions of $FeCl_3{\times}6\,H_2O$, $Ni(NO_3)_2{\times}6\,H_2O$, $Co(NO_3)_2{\times}6\,H_2O$ (all ≥ 99.0%, Sinopharm Group Co. Ltd.) were mixed in their stoichiometric ratio and continuously stirred at 80 °C for 1 h. In the next step, NaOH solution was slowly added into the precursor solution mixture with constant stirring and pH was adjusted to ~12. After continued stirring for 1 h, the solution was naturally cooled to room temperature and the obtained product was filtered and washed several times with distilled water until the pH decreased to ~7 to remove the unwanted salt residues and other impurities. Subsequently, the precipitated particles were then dried at 100 °C for 24 h to obtain the dry powder. After that, the powder was ground, then mixed with polyvinyl alcohol (PVA) and filtered through sieve. Afterwards, the particles were pressed into pellet with the diameter of 10 mm and the thickness of 1 mm, and finally sintered at 1000 °C for 8 h to obtain the required ceramics.

The crystal structure of the prepared ceramics was investigated at room temperature by X-ray diffraction (XRD, D/max 2500, Rigaku, Japan) using Cu-K$\alpha$ radiation ($\lambda$ = 1.5406 Å) in the $2\theta$ range from 20° to 70°. Scanning electron microscopy (FE-SEM, JSM-7800F, JEOL, Japan) was used to observe the surface morphology of the ceramics. The dielectric properties of the samples were characterized by using an impedance analyser (HP4980A, Agilent, USA). The relative dielectric constant ($\varepsilon_r$) can be calculated from the capacitance based on the following equation:

$$\varepsilon_r = \frac{C \cdot d}{\varepsilon_0 \cdot S} \tag{1}$$

where $C$ is the measured capacitance, $d$ is the thickness of the samples, $\varepsilon_0$ is the vacuum dielectric constant ($8.85\times10^{-12}$ F/m) and $S$ is the effective area of the electrode on the samples. Room temperature magnetic hysteresis ($M$-$H$) loops were determined by using a vibrating sample magnetometer (VSM, VSM100~500) with maximum magnetic field of ±1.5 T.

## III. Results and discussion

### 3.1. Microstructure

The X-ray diffraction patterns of the prepared ceramics are shown in Fig. 1a. It can be found that all the samples show good crystallinity with different Co content, indicating a poly-crystalline spinel structure without any discernible secondary phases. Besides, it can be clearly seen from Fig. 1b that the diffraction peaks shift to lower angle region with the increase of Co content, which demonstrates that the interplanar distance and lattice constant increase with Co increasing. The lattice parameter $a$ for individual compositions can be calculated from the most intense reflection peak 311 of the cubic spinel structure by using the formula [28]:

$$a = d\sqrt{h^2 + k^2 + l^2} \tag{2}$$

where $h$, $k$, and $l$ are the Miller indices. It can be found that the lattice parameter increases from 8.302 Å to

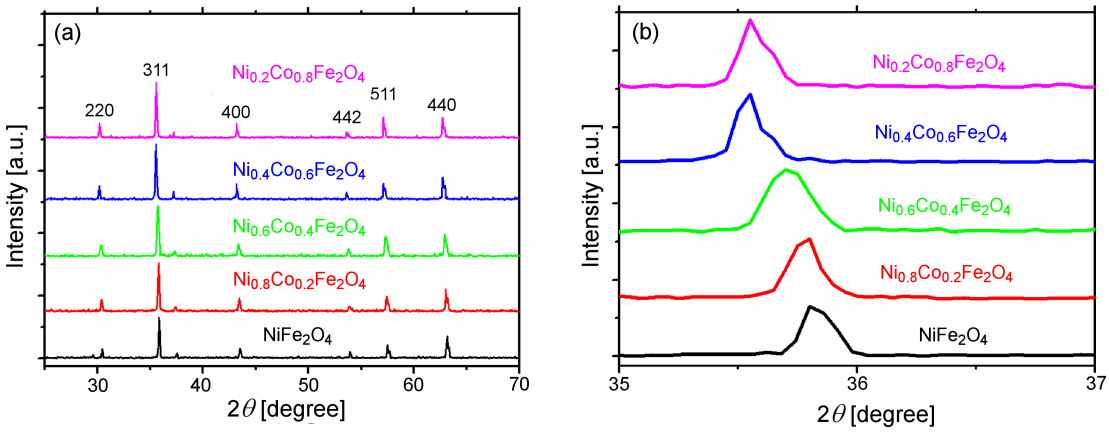


**Figure 1. XRD patterns of $Ni_{1-x}Co_xFe_2O_4$ ceramics (a) and magnified $2\theta$ region with 311 peak (b)**

8.411 Å when the Co concentration increases from $x$ = 0 to $x$ = 0.8. This increased lattice parameter with the increase in $Co^{2+}$ ion concentration is attributed to the replacement of $Ni^{2+}$ ions with smaller radius (~0.63 Å) by $Co^{2+}$ ions with larger radius (~0.78 Å) in the host lattice of nickel ferrite [29]. Therefore, we argue that $Co^{2+}$ ions with relative larger ionic radius have substituted $Ni^{2+}$ ions with smaller ionic radius, and this resulted in the expansion of the crystal lattice.

In addition to the crystal structure, Co-doping can play a role in the modulation of the surface morphology and the grain size. Figure 2 shows the surface morphology of $Ni_{1-x}Co_xFe_2O_4$ ceramics with different Co content. It can be found that all the samples show relatively high density, while the surface of the ceramics consists of some grains with relatively inhomogeneous distribution of grain size; the average grain size varies from 2 to 5 μm. The relative densities of $Ni_{1-x}Co_xFe_2O_4$ ceramics, where $x$ = 0, 0.2, 0.4, 0.6, 0.8, are 94.2, 94.7, 95.1, 95.6 and 95.8% TD, respectively. This result indicates that the addition of Co ion can improve the sinterability. Furthermore, the mean grain size shows slightly decreased trend with Co addition. This clearly shows that the substitution of $Ni^{2+}$ with $Co^{2+}$ ion has a direct influence on the microstructure of the ceramics. It demonstrates that the addition of Co can effectively inhibit the grain growth of $Ni_{1-x}Co_xFe_2O_4$ ceramics. $Co^{2+}$ ions in the high temperature sintering process can dissolve into $NiFe_2O_4$ lattice and replace $Ni^{2+}$ ions and thus lead to lattice distortion. In addition, $Co^{2+}$ ions are easily segregated on the grain boundary, hindering the mobility of the grain boundary and inhibiting the grain growth.

### 3.2. Dielectric properties

The changes in the dielectric constant of the Co-doped $NiFe_2O_4$ ceramics as a function of frequency are shown in Fig. 3. One can see that the dielectric constant shows non-monotonic variation with Co content. It increases firstly, then decreases and finally it increases again in the low frequency range ($f < 10^5$ Hz). The minimal dielectric constant is obtained in the pure $NiFe_2O_4$ sample while the maximum occurs at $x$ = 0.8. On the

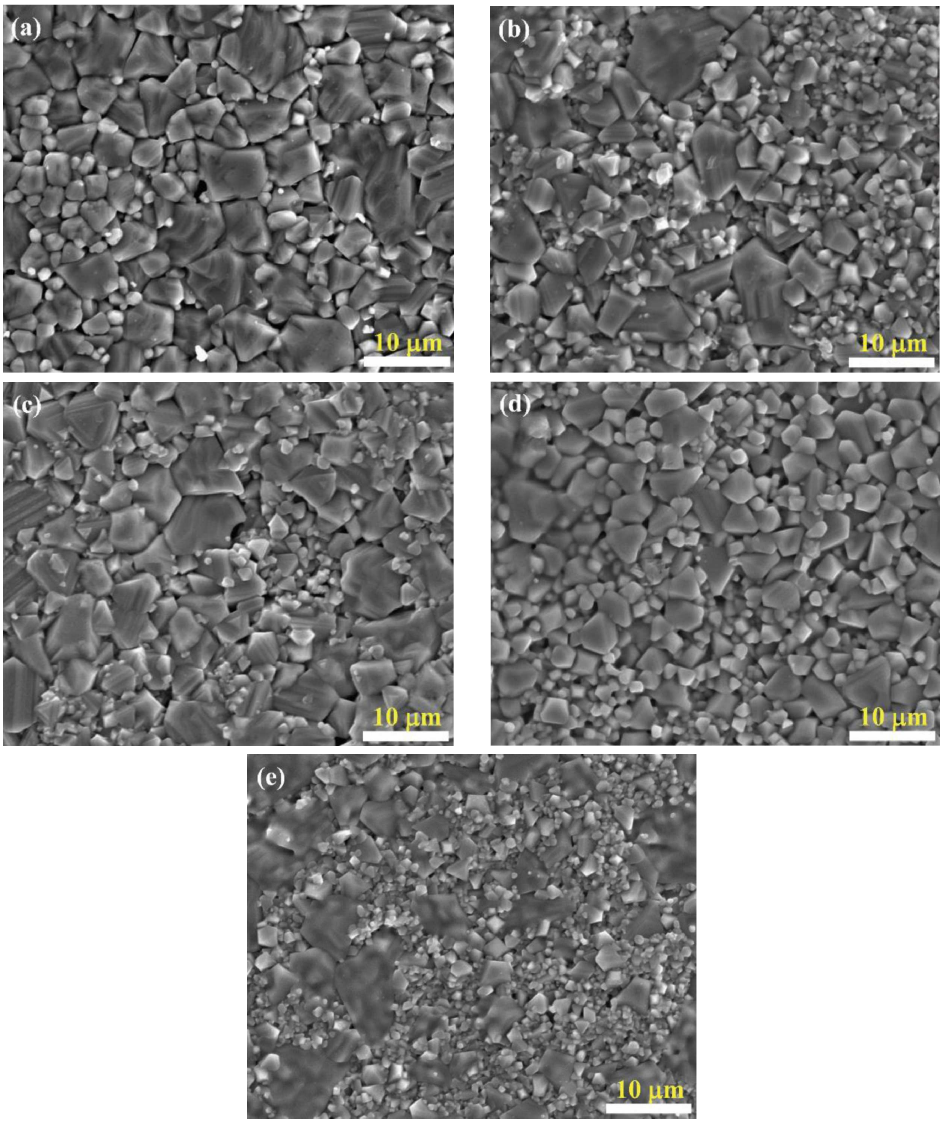


**Figure 2. SEM images of $Ni_{1-x}Co_xFe_2O_4$ ceramics: a) $x$ = 0, b) $x$ = 0.2, c) $x$ = 0.4, d) $x$ = 0.6 and e) $x$ = 0.8**

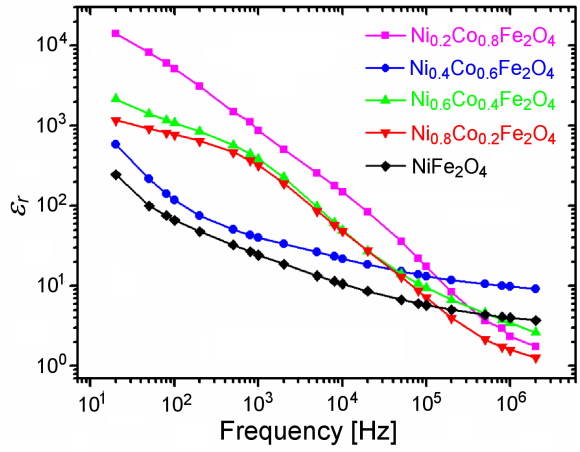


**Figure 3. Frequency dependence of the dielectric constant of $Ni_{1-x}Co_xFe_2O_4$ ceramics**

contrary, when the frequency is larger than $10^5$ Hz, the permittivity shows another variation with Co ion, i.e. it decreases and then increases with Co concentration and eventually it decreases again. When the content of Co ion is 0.2, the corresponding dielectric constant is the minimal, while the maximal dielectric constant is observed in the sample when $x = 0.6$. In addition, it is very obvious that all the dielectric constants of all the samples decrease quickly in the low frequency range and this decreased trend becomes slower when the frequency is high. Moreover, it is very clear that the dielectric constants of the samples $Ni_{0.8}Co_{0.2}Fe_2O_4$ and $Ni_{0.6}Co_{0.4}Fe_2O_4$ in the measured range of 20 Hz–2 MHz are more stable than that of other doped and undoped samples.

The frequency dependence of the dielectric constant can be explained based on the different polarization mechanisms under different measuring frequency. The polarization mechanism includes displacement polarization, space charge polarization and turning-direction polarization. The relaxation time of displacement polarization ($\sim 10^{-13}$ s) is so short that it can be considered to be independent of the test frequency (20 Hz–2 MHz). Therefore, the displacement polarization contribution to the dielectric constant is also independent of the test frequency, and the dielectric constant should show perfect frequency stability. In contrast, the relaxation time of space charge polarization and turning-direction polarization is roughly in the range of $10^{-2}$–$10^{-6}$ s, which is comparable to that of the examined frequency range. As a consequence, in the low frequency, the polarization process can be fully established so that large dielectric constant can be obtained. However, the polarization process cannot be entirely formed in the high frequency range, thus only smaller dielectric constant can be observed. In brief, as more and more polarization processes cannot be established with increase in the frequency, the dielectric constant decreases monotonically with the frequency increase in the whole frequency range. The better the frequency stability of the dielectric constant, the lower the relaxation polarization (including space charge polarization and turning-direction polarization) should be. The relaxation polarization is often induced by space charge, impurity, defects such as oxygen vacancy, weekly bound charge and so forth. The reason that there is a broad pick in frequency dependence of dielectric constant for the samples $Ni_{0.8}Co_{0.2}Fe_2O_4$ and $Ni_{0.6}Co_{0.4}Fe_2O_4$ at about 1 kHz is that there are less space charges and oxygen vacancies in the two samples. Although this standpoint cannot be directly concluded from the XRD and SEM images, it might be that Co doping has such influence on the crystal structure and grain size of $NiFe_2O_4$ ceramics that moderate addition of $Co^{2+}$ ions may result in the reduction of defects in the samples to some extent. In general, defects and impurities are directly related to the electric properties.

### 3.3. Magnetic properties

Figure 4 shows room temperature magnetic hysteresis loops obtained from VSM measurement of the $Ni_{1-x}Co_xFe_2O_4$ ceramics. It can be seen that all $Ni_{1-x}Co_xFe_2O_4$ ceramics exhibit hard ferromagnetic behaviour. Furthermore, the hysteresis loops of the samples present smooth hysteresis, indicating single phase like magnetic material behaviour. This behaviour reveals that the $Co^{2+}$ is tailored to $NiFe_2O_4$ lattices perfectly. The saturation magnetization ($M_s$), coercive field ($H_c$) and remnant magnetization ($M_r$) are listed in Table 1. It is found that the values of $M_s$ and $M_r$ increase monotonically with increasing Co content. These increases can be explained in terms of the existence of both $Ni^{2+}$ and $Co^{2+}$ ions, which could cause exchange interaction between them. Another important reason is attributed to a larger magnetic moment of $Co^{2+}$ ($3\mu_B$) at the octahedral sites as compared to the $Ni^{2+}$ ($2\mu_B$).

In an ideal spinel lattice, on one hand, the magnetization is generally given by the different moments of the tetrahedral A sites and the octahedral B sites. If the magnetic moments of the $Fe^{3+}$ ions at the A and B sites are entirely equal and opposite, they can compensate each other. On the other hand, the magnetization naturally depends on the distribution of magnetic and non-

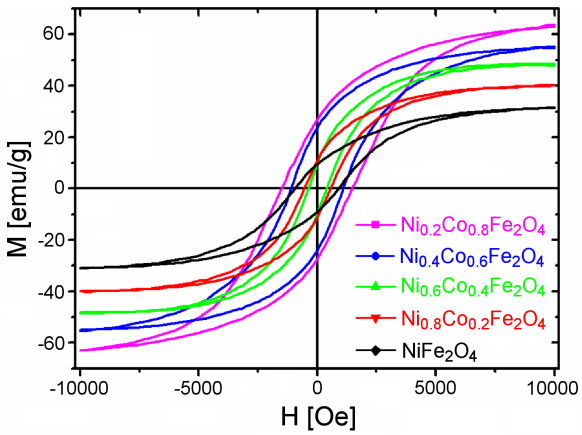


**Figure 4. Hysteresis loops of $Ni_{1-x}Co_xFe_2O_4$ ceramics**

**Table 1. The saturation magnetization, remnant magnetization and coercive field of $Ni_{1-x}Co_xFe_2O_4$ ceramics**

| $Ni_{1-x}Co_xFe_2O_4$ | $x = 0$ | $x = 0.2$ | $x = 0.4$ | $x = 0.6$ | $x = 0.8$ |
|---|---|---|---|---|---|
| $M_s$ [emu/g] | 31.305 | 40.177 | 48.516 | 54.986 | 63.125 |
| $M_r$ [emu/g] | 9.455 | 9.931 | 11.0195 | 23.748 | 26.942 |
| $H_c$ [Oe] | 893.87 | 560.60 | 391.45 | 1093.72 | 1475.56 |

magnetic ions in the A and B sites of the ferrite lattice. In spinel $NiFe_2O_4$ and $CoFe_2O_4$ lattices all the tetrahedral sites (A) and the octahedral sites (B) show an antiparallel arrangement of magnetic moments. Therefore, one assumes if $Fe^{3+}$ (with a magnetic moment of $5\mu_B$) is evenly distributed between the tetrahedral and octahedral sites, this will give a net magnetic moment of $2\mu_B$ per molecule for $NiFe_2O_4$ and $3\mu_B$ per molecule for $CoFe_2O_4$. Therefore, the saturation magnetization of Co-doped $NiFe_2O_4$ ceramics will increase with the Co concentration because of the larger magnetic moment of Co ions as compared to that of Ni ions. Furthermore, the magnetic interaction was tended to be weaker in a disordered phase. As a consequence, the grain boundary density decreases with increasing the grain size, which in turn increases the magnetization.

In addition, the coercive field presents a non-monotonic dependency relationship with the Co concentration. The maximal value of coercive field has $Ni_{0.2}Co_{0.8}Fe_2O_4$ ceramics because of the hard behaviour of cobalt ferrite. The high value of $H_c$ could be interpreted in the light of one ion model [30]. The minimal coercive field occurs in $Ni_{0.6}Co_{0.4}Fe_2O_4$ ceramics and may be explained by the grain size effect (due to the enhancement of the effective anisotropy constant, $K_{eff}$). The contribution of the surface anisotropy constant ($K_S$) can be described as [31]:

$$K_{eff} = K_{bulk} + \frac{6K_S}{d} \tag{3}$$

where $d$ is the diameter of grains. Therefore, the surface and its associated anisotropies can play very important role in case of nanosize grains. The room temperature coercivity values for various Co concentrations show that the *M-H* curves of all the samples do not entirely saturate even at the applied field of 10 kOe, especially when the concentration of Co is very high. Hence, the saturation of magnetization is difficult to obtain due to the surface canted spins because of the broken exchange bonds at the surface of nanograins. We can see from Fig. 4 that the coercivity of the prepared ceramics decreases firstly and then increases with increasing Co concentration, while the grain size decreases slightly with Co concentration. It is obvious that the variation of coercivity with increasing Co concentration may be attributed to the higher magneto-crystalline anisotropy of $Co^{2+}$ as compared to that of $Ni^{2+}$ ions which in turn can lead to higher coercive field according to the Stoner Wolfforth model for nanoparticles ($H_c = 2K/M_s$). However, according to our results, although all grain sizes are in the order of a few μm, these grains are large enough to support the domain walls, and thus the coercivity of these grains could be reduced by magnetization reversal through the domain wall [32]. The grain sizes show monotonic variation with the concentration of Co, while the coercive field does not show monotonic variation. Therefore, only the grain size effect cannot be used to explain the variation of coercivity. Furthermore, it is very strange that the pure $NiFe_2O_4$ shows hard magnetic behaviour. The coercivity (~893.87 Oe) of $NiFe_2O_4$ is so high that the size effect cannot be solely used to interpret this unusual phenomenon. Many factors, for example, magnetic anisotropy (including anisotropy such as magnetic crystals, induction, shape and stress), impurities, pores, defects etc., have major effect on the coercivity. The coercivity determined by boundaries can be expressed as:

$$H_c \approx 3\frac{\gamma_w}{M_s}\frac{1}{D} \tag{4}$$

where $\gamma_w$ is the domain wall energy, and $M_s$ is the saturation magnetization. $\gamma_w$ can be stated as:

$$\gamma_w \approx \sqrt{\frac{k \cdot T_c \cdot K_1}{a}} \tag{5}$$

Therefore, $H_c$ can be expressed as follows:

$$H_c \approx \frac{\sqrt{\frac{k \cdot T_c \cdot K_1}{a}}}{M_s}\frac{1}{D} \tag{6}$$

where $k$ is the Boltzmann constant, $K_1$ is the magnetocrystalline anisotropy, $T_c$ is the Curie temperature, and $a$ is the lattice constant. In the case of low Co content, the grain size plays an important role, thus $H_c$ is slightly decreased [33]. Nevertheless, with the increase of Co content, such behaviour is also consistent with the effect of the grain size on the magnetic properties of nanoscale materials, thus anisotropy constant and the magnetic magnitude are more and more important. Coercive field presents the increased trend gradually. The high value coercivity may be enhanced by the anisotropic constant with increasing Co content [34]. In other words, the size effect may be inadequate to account for the hard magnetic behaviour of the pure $NiFe_2O_4$.We speculate that the shape of grains, defects, impurities and holes in the sample can also play important roles in the coercive field. Therefore, further work is needed in the next investigation process.

## IV. Conclusions

$Ni_{1-x}Co_xFe_2O_4$ ($x$ = 0, 0.2, 0.4, 0.6, 0.8) ceramics were synthesized by chemical co-precipitation method and sintered at 1000 °C. X-ray powder diffraction con-

firms the formation of the single-phase crystalline structure without any trace of impurity. The lattice parameter increases with increased Co content because of the larger ionic radius of $Co^{2+}$ compared with that of $Ni^{2+}$. The density increases with Co-doping, whereas the average grain size calculated from SEM varies in the range of 2–5 μm and decreases slightly with Co concentration.

The impedance spectroscopy confirms that the dielectric constant increases with Co content, while it presents relatively stable values as a function of frequency in a certain extent of Co doping. In addition, incorporation of cobalt in the spinel nickel ferrite structure can enhance the saturation magnetization and remnant magnetization because of the stronger magnetism of $CoFe_2O_4$ compared to $NiFe_2O_4$ material. In the case of 40 at.% Co-doping, this larger magnetization and lower coercivity than the pure nickel ferrite ceramics indicates the size effect and presents the obvious modulation effect of Co-doping on nickel ferrites. At higher Co-doping, the anisotropy constant and the magnitude of magnetic moment begin to be the main factors, so that the coercivity shows a gradual upward trend. The grains shape, defects, impurities and holes exhibit considerable effect on the unusually large coercive field in the prepared ceramics. Our results propose a feasible approach to improve the magnetic properties in nickel ferrite ceramics.

**Acknowledgement:** The present work has been supported by the Natural Science Foundation of Chongqing (CSTC2018jcyjAX0416, CSTC2016jcyjA0175, CSTC2016jcyjA0349), the Young Scientific and Technological Research Program of Chongqing Municipal Education Commission (KJQN201801509), the Excellent Talent Project in University of Chongqing (Grant No. 2017-35), the Science and Technology Innovation Project of Social Undertakings and Peoples Livelihood Guarantee of Chongqing (Grant No. cstc2017shmsA0192), the Program for Innovation Teams in University of Chongqing, China (Grant No. CXTDX201601032), the Foundation of Chongqing University of Science & Technology (CK2015B05, CK2015Z13), the Latter Foundation Project of Chongqing University of Science & Technology (CKHQZZ2008002) and the Scientific & Technological Achievements Foundation Project of Chongqing University of Science & Technology (CKKJCG2016328).

## References

1. A.L. Lopes-Moriyama, V. Madigou, C.P. deSouza, C. Leroux, "Controlled synthesis of $CoFe_2O_4$ nanooctahedra", *Powder Technol.*, **256** (2014) 482–489.
2. M. Hashim, A. ShalendraKumar, B.H. Koo, S.E. Shirsath, E.M. Mohammed, R.K. Kotnala, H.K. Choi, H.C. Ravi Kumar, "Structural, electrical and magnetic properties of Co-Cu ferrite nanoparticles", *J. Alloys Compd.*, **518** (2012) 11–18.
3. S.T. Assar, H.F. Abosheiasha, M.K. ElNimr, "Comparison study of the magnetic permeability and dc conductivity of Co-Ni-Li ferrite nanoparticles and their bulk counterparts", *J. Magn. Magn. Mater.*, **354** (2014) 1–6.
4. A.A. Sattar, H.M. EL-Sayed, I.A. Lsuqia, "Structural and magnetic properties of $CoFe_2O_4$/$NiFe_2O_4$ core/shell nanocomposite prepared by the hydro thermal method", *J. Magn. Magn. Mater.*, **395** (2015) 89–96.
5. K.W. Zhou, L.Q. Qin, X.H. Wu, W.W. Wu, Y.X. Shen, Y.L. Tian, J.Y. Lu, "Structure and magnetic properties of manganese-nickel ferrite with lithium substitution", *Ceram. Int.*, **41** (2015) 1235–1241.
6. S.S. Khot, N.S. Shinde, N. Basavaiah, S.C. Watawe, M.M. Vaidya, "Magnetic properties of LiZnCu ferrite synthesized by the microwave sintering method", *J. Magn. Magn. Mater.*, **374** (2015) 182–186.
7. R.L. Gao, J. Li, S.N. Han, B.C. Wen, T.Z. Zhang, H. Miao, Q.M. Zhang, "Magnetisation behaviour of mixtures of ferrofluids and paramagnetic fluids with same particle volume fractions", *J. Exp. Nanosci.*, **7** (2012) 282–289
8. L.Q. Qin, M.L. Gao, W.W. Wu, S.Q. Ou, K.T. Wang, B. Liu, X.H. Wu, "$Co_{1-x}Mg_xFe_2O_4$ magnetic particles: preparation and kinetics research of thermal transformation of the precursor", *Ceram. Int.*, **40** (2014) 10857–10866.
9. A.R. Wang, J. Li, R.L. Gao, "The structural force arising from magnetic interactions in polydisperse ferrofluids", *Appl. Phys. Lett.*, **94** (2009) 212501.
10. W.W. Wu, J.C. Cai, X.H. Wu, K.T. Wang, Y.M. Hu, Q. Wang, "Nanocrystalline $Cu_{0.5}Zn_{0.5}Fe_2O_4$: Preparation and kinetics of thermal decomposition of precursor", *J. Supercond. Nov. Magn.*, **26** (2013) 3523–3528.
11. S.N. Han, J. Li, R.L. Gao, T.Z. Zhang, B.C. Wen, "The modification effect in magnetization behaviors for $CoFe_2O_4$-p-$NiFe_2O_4$ binary ferrofluids", *Appl. Phys A*, **98** (2010) 179–183
12. R.S. Melo, F.C. Silva, K.R.M. Moura, A.S. de Menezes, F.S.M. Sinfrônio, "Magnetic ferrites synthesised using the microwave-hydro thermal method", *J. Magn. Magn. Mater.*, **381** (2015) 109–115.
13. A.T. Raghavender, "Synthesis and characterization of cobalt ferrite nanoparticles", *Sci. Technol. Arts Res. J.*, **2** (2013) 1–4.
14. Q. Song, Z.J. Zhang, "Shape control and associated magnetic properties of spinel cobalt ferrite nanocrystals", *J. Am. Chem. Soc.*, **126** [19] (2004) 6164–6168.
15. V. Sepelak, I. Bergmann, A. Feldhoff, P. Heitjans, F. Krumeich, D. Menzel, F.J. Litterst, S.J. Campbell, K.D. Becker, "Nanocrystalline nickel ferrite, $NiFe_2O_4$: mechano synthesis, nonequilibrium cation distribution, canted spin arrangement, and magnetic behavior", *J. Phys. Chem. C*, **111** (2007) 5026–5033.
16. K. Nejati, R. Zabihi, "Preparation and magnetic properties of nanosize nickel ferrite particles using hydro thermal method", *Chem. Cent. J.*, **6** (2012) 23–29.
17. F. Genc, B. Unal, A. Baykal, H. Sozeri, "Electrical properties of Mn-doped $Ni_xZn_{0.9-x}Fe_2O_4$ particles", *J. Supercond. Nov. Magn.*, **28** (2015) 1055–1064.
18. A.T. Nelson, J.T. White, D.A. Andersson, J.A. Aguiar, K.J. Mcclellan, D.D. Byler, M.P. Short, C.R. Stanek, "Thermal expansion, heat capacity, and thermal conductivity of nickel ferrite ($NiFe_2O_4$)", *J. Am. Ceram. Soc.*, **97** [5] (2014) 1559–1565.
19. Y. Zhou, W. Chen, Y.X. Shen, X.H. Wu, W.W. Wu, J. Wu, "Lattice strains and magnetic properties evolution of copper-magnesium ferrite with lithium substitution", *J. Magn. Magn. Mater.*, **396** (2015)198–203.

20. Z. Cvejic, E. Đurdic, G.I. Ivandekic, B. Bajac, P. Postolache, L. Mitoseriu, V.V. Srdic, S. Rakic, "The effect of annealing on microstructure and cation distribution of $NiFe_2O_4$", *J. Alloy. Compds.*, **649** (2015) 1231–1238.
21. X. Shen,Y.X. Wang, L.Q. Lu, Y.L. Chen, Y. Xia, Y.H. Li, "Preparation and optical properties of $TiO_{2-x}N_x/Ni_{0.5}Zn_{0.5}Fe_2O_4$ core-shell nanocatalyst from sol-gel-hydrothermal process", *J. Sol-Gel Sci. Technol.*, **54** (2010) 340–346.
22. V.C. Nguyen, T.K.N. Huynh, "Reusable nanocomposite of $CoFe_2O_4$/chitosan-graft-poly (acrylicacid) for removal of Ni(II) from aqueous solution", *Adv. Nat. Sci. Nanosci. Nanotechnol.*, **5** (2014) 025007.
23. R. Bujakiewicz-Korońska, Ł. Hetmańczyk, B. Garbarz-Glos, A. Budziak, A. Kalvane, K. Bormanis, K. Drużbicki, "Low temperature measurements by infrared spectroscopy in $CoFe_2O_4$ ceramic", *Cent. Eur. J. Phys.*, **10** [5] (2012) 1137–1143
24. G.N. Chavan, P.B. Belavi, L.R. Naik, B.K. Bammannavar, K.P. Ramesh, S. Kumar, "Electrical and magnetic properties of nickel substituted cadmium ferrites", *Int. J. Sci. Technol. Res.*, **2** [12] (2013) 82–89.
25. A.L. Ortega, M. Estrader, G.S. Alvarez, A.G. Roca, J. Nogués, "Applications of exchange coupled bi-magnetic hard/soft and soft/hard magnetic core/shell nanoparticles", *Phys. Rep.*, **553** (2015) 1–44.
26. R. Chen, M.G. Christiansen, P. Anikeeva, "Maximizing hysteretic losses in magnetic ferrite nanoparticles via model-driven synthesis and materials optimization", *ACS Nano*, **7** (2013) 8990–9000.
27. M. Coşkun, M. Korkmaz, T. Fırat, G.H. Jaffari, S.I. Shah, "Synthesis of $SiO_2$ coated $NiFe_2O_4$ nanoparticles and the effect of $SiO_2$ shell thickness on the magnetic properties", *J. Appl. Phys.*, **107** (2010) 09B523.
28. M. Goerge, A. Mary John, S.S. Nair, P.A. Joy, M.R. Anantharaman, "Finite size effects on the structural and magnetic properties of sol-gel synthesized $NiFe_2O_4$ powders", *J. Magn. Magn. Mater.*, **320** (2006) 190–195.
29. J. Xiang, Y. Chu, X. Zhang, X. Shen, "Magnetic and microwave absorption properties of electrospun $Co_{0.5}Ni_{0.5}Fe_2O_4$ nanofibers", *Appl. Surf. Sci.*, **263** (2012) 320–325.
30. P. Sivakumar, R. Ramesh, A. Ramanand, S. Ponnusamy, C. Muthamizhchelvan, "Preparation and properties of $NiFe_2O_4$ nanowires", *Mater. Lett.*, **66** (2012) 314–317.
31. C.R. Vestal, Z.J. Zhang. "Synthesis and magnetic characterization of Mn and Co spinel ferrite-silica nanoparticles with tunable magnetic core", *Nano Lett.*, **3** [12] (2012) 1739–1743.
32. K. Haneda, H. Kojima, A.H. Morrish, "Magnetic excitations in small $NiFe_2O_4$ particles", *J. Magn. Magn. Mater.*, **31** (1983) 951–952.
33. R.H. Yu, S. Basu,Y. Zhang, A.P. Majidi, J.Q. Xiao, "Pinning effect of the grain boundaries on magnetic domain wall in FeCo-based magnetic alloys", *J. Appl. Phys.*, **85** (1999) 6655–6659.
34. K. Maaz, S. Karim, A. Mashiatullah, J. Liu, M.D. Hou, "Structural analysis of nickel doped cobalt ferrite nanoparticles prepared by coprecipitation route", *Physica B*, **404** (2009) 3947–3951.